Oct 18th, 12:00 AM

Behavior and Failure Mechanism of Composite Slabs

J. J. Roger Cheng

Michael C. H. Yam

E. B. Davison

Twelfth International Specialty Conference on Cold-Formed Steel Structures
St. Louis, Missouri, U.S.A., October 18-19, 1994.

BEHAVIOR AND FAILURE MECHANISM OF COMPOSITE SLABS

J.J. Roger Cheng[1], Michael C.H. Yam[2] and E.B. Davison[3]

SUMMARY: The behavior of a composite slab using a 636 deck profile was investigated experimentally. Twenty-three one-way slab tests and twenty-four pull-out tests were performed. It was found that the behavior and shear bond load of the composite slab were significantly affected by the depth of the embossment shear key. The average shear stress from the pull-out tests was generally lower than that of the one-way slab tests due to a lack of the transverse load effects which influenced the frictional resistance between the concrete slab and the steel deck.

INTRODUCTION

During the last two decades, research towards the development of effective flooring systems has resulted in a system based on the composite action of a concrete slab and a cold-formed steel deck. This deck serves both purposes of providing the formwork for the concrete slab and acting as the tensile reinforcement for the composite slab system. To achieve the desirable composite action, shearing forces have to be transferred between the concrete slab and the steel deck. This is usually accomplished by the mechanical interlocking devices rolled into the surface of the steel deck such as embossments and indentations.

The design of composite slab system is currently based on the results of performance tests for a particular steel deck profile. Two types of steel deck profiles; namely, 636 (depth = 38 mm) and 324 (depth = 76 mm) decks produced by INDAL METAL LTD in Edmonton, Alberta were tested in the University of Alberta to investigate the parameters that significantly affect the shear bond strength and characteristics of the composite slab system. For this particular paper, only the findings for 636 decks are presented. A total of 23 simply supported composite slabs were tested according to the CSSBI S2-85 specification (revised 1988). The shear-bond coefficients K_5 and K_6 were also evaluated for the 636 decks. A number of test variables were also included in this testing program in order to examine the behavioral characteristics of the composite slab system. In addition, two series of pull-out tests were also conducted with the 636 deck profile to investigate the mechanical interlocking strength of the decking and an attempt was made to correlate the pull-out test results with the standard simply supported slab test results. A schematic of typical 636 deck is shown in Fig. 1.

[1] Associate Professor of Civil Engineering, University of Alberta, Edmonton, Alberta, Canada.
[2] Grad. student, Dept. of Civil Engineering, University of Alberta, Edmonton, Alberta, Canada.
[3] President, RSD Engineering Inc., Edmonton, Alberta, Canada.

EXPERIMENTAL PROGRAM

Scope

For the standard slab tests, the experimental program consists of 2 phases of testing. Phase I testing program aims at investigating the shear bond characteristics of the composite slab system. A total of 11 tests were performed on the 636 decks with variables such as shear span length, types of shear keys (embossment and indentation), two deck positions: normal and inverted (normal - the usual deck orientation with the smaller flanges located at the bottom, and inverted - the deck is used in an upside down orientation with the larger flanges located at the bottom), and two zinc surface coatings (G90 - 275g/m^2 and S - 75g/m^2). The second phase of the experimental program is employed to evaluate the shear-bond coefficients of the 636 decks with two surface coatings, G90 and S. The 636 decks used in the second phase were manufactured by a new set of dies which produced a deeper chevron shear key than that of the first phase. A total of 12 tests were performed in the second phase with six tests for each surface coating. According to CSSBI S2-85 (revised 1988) a minimum of 4 tests are required to generate the K_5 and K_6 shear-bond coefficients with 2 tests each on the maximum shear-bond resistance and the minimum shear-bond resistance. Two additional tests were performed to verify the shear-bond coefficients.

For the pull-out tests, the experimental program consists of 2 phases of testing. The first phase of the testing program investigates the variables such as the pulling direction relative to the chevron shear keys pointing direction, the type of surface coating, the deck position and the shear key type (embossment vs. indentation). The second phase of the program examines the effects of the depth of the shear keys. In particular, all the specimens are normal deck position and with embossment shear keys. The two surface coating conditions (G90 and S) were also included as the test variable.

Specimen Description

The average measured dimensions of the steel deck panels are presented in Tables 1 and 2 for Phase I and II, respectively. The specimen designation system for the testing program basically followed Schuster's system (1990) with minor modifications to account for deck positions, type of chevron shear keys and surface coatings as follow:

example: Specimen Designation : 636-22-100-675-NE-G90

636 - steel deck type identification
22 - gauge number
100 - overall specimen depth, h (mm)
675 - shear span length, L' (mm)
N - normal deck position (I - inverted deck position)
E - embossment (I - indentation)
G90 - steel deck surface coating

As shown in the tables that the maximum shear span length considered was 900 mm and the minimum shear span length was 450 mm and a intermediate shear span length of 675 mm was used for both Phase I and II testing programs. For Phase I testing program, only one slab thickness of 100 mm was considered. For Phase II testing program, however, three slab thicknesses of 100 mm, 125 mm and 150 mm were used. As can be seen from Tables 1 that the steel deck thickness (t) for majority of the specimens were very close to the nominal value of 0.76 mm. However, the average measured steel deck thickness of the G90 specimens in Phase II was

0.81 mm. As shown in Tables 1 and 2, the depth of the chevron shear keys for the Phase II specimens was significantly larger than that of the Phase I specimens. Continuous supports for specimens were provided during casting. The specimens were moist cured for seven days and then air cured for at least an additional 21 days before testing. Concrete cylinders were also cast for ancillary tests.

The dimensions and designations of the pull-out specimens are shown in Table 3. The designation of the specimens used in this series of tests is similar to that of the one-way slab tests with the first alphabet represents the deck position and the second alphabet represents the types of chevron key. Three types of specimens were tested in this series, namely; NE, NI, and II. As can be seen from Table 3 that the pulling and key directions were varied for each type of specimen (NE, NI and II) to investigate the effects of chevron key direction on the shear bond strength of the specimen. The pulling direction of the steel deck is indicated by an arrow and the direction of the chevron shear keys is indicated by a double arrow head as shown in Fig. 2. It should be noted that the Phase II specimens have a significantly deeper chevron key than that of the Phase I. Each specimen has one replication to confirm the test results.

Test Setup and Instrumentation

A schematic of the test setup is shown in Fig 3. As can be seen from this figure, the MTS loading system was used to applied the transverse loads to the specimen. Stroke control was used in the MTS loading system to monitor the load deflection behavior of all the specimens. Roller and rocker assembly was used to support the specimen and the distributing beam as shown in Fig. 2. Fiber-boards were placed under the rectangular hollow sections for even load distribution onto the concrete slab. Linear variable displacement transducers (LVDTs) were located at each end of the specimen to measure the end slip. Vertical separation under the line load was also monitored by LVDTs. A cable transducer was attached to the midspan of the specimen to measure centerline deflection. Load cells were placed under the ends of the distributing beam (RHS sections) to record the actual applied load to the specimen. All the readings from the LVDTs, load cells and MTS load and stroke were recorded directly by a data acquisition system. Load was applied slowly to the specimen at various load levels. LVDTs readings, MTS load and stroke and load cell readings were recorded after each load increment. Concrete cracks were recorded and marked on the specimens. The test was terminated when the specimen reached the ultimate load and unloading occurred or the steel deck was completely disengaged from the concrete slab.

A schematic of the pull-out test setup is shown in Fig. 4. As can be seen from this figure, two steel plates were bolted to the top and bottom of the steel deck to transfer the pulling force provided by the hydraulic jack system which in turn bear against the concrete slab through a set of end plates. This test setup produced a self-equilibrating system which supplied the push-and-pull action required by the push-out tests. The pressure in hydraulic jacks was supplied by a hand oil pump. The steel rods attached to the hydraulic jacks were placed at the center of the two steel plates to avoid eccentricity as shown in Fig. 4. A LVDT was attached to the end of the specimen to record end slip occurred during the test. Load was applied steadily to the specimens by pumping the hydraulic jack continuously until the concrete slab rode over and up the steel deck. All the data were recorded automatically during the entire loading stage by the data acquisition system.

Ancillary Tests

Tension coupons were cut from the top and bottom flanges of the steel decks in the longitude direction. Coupons were fabricated and tested according to ASTM A370 (1992). Standard concrete cylinders were made during casting of the composite slabs. Concrete cylinders were tested according to CSA A23.3 M84 (1984).

TEST RESULTS

Simply Supported Composite Slab

The steel deck static yield strength, the concrete strength and the ultimate loads of the specimens are shown in Tables 4 and 5 for test Phases I and II, respectively. The test results of each test phase will be presented individually as follow:

Phase I

In general, all the Phase I specimens experienced shear-bond failure. Major diagonal cracks were observed at the shear span originated from the point of loading. Significant end slips were recorded at ultimate for all the specimens, however, negligible vertical separation was recorded prior to ultimate load. The shear bond failure usually occurred in the shear span where the chevron embossment pointed away from the end of the specimen. This particular observation will be examined in detail by the pull-out test results. It can be seen from Table 4 that the ultimate load of the specimens was significantly affected by the type of surface coating. In general, the G90 specimen yielded a lower ultimate load but exhibited a more ductile load deflection behavior. For the S coating specimens a higher ultimate load and relatively brittle failure were observed. The type of shear keys (embossment vs. indentation) seems to have minor effects on the ultimate load and load deflection behavior of the specimens when comparing the test results of the G90 specimens. On the contrary, the test results of the S specimens indicated that the ultimate load was increased when either embossment or inverted deck was used. This contradiction will be examined in the following section of discussion of test results. Table 4 illustrates that the ultimate load of the specimens increased with decreasing shear span.

Phase II

The test results of Phase II are shown in Table 5. It should be noted that the chevron shear keys in the steel deck for this testing phase were manufactured by a new set of dies which produced deeper shear keys. When comparing the depth of the shear keys for this phase to that of Phase I a significant increase in shear key depth is observed. This increase in shear key depth contributed to the general increase in the ultimate load of the Phase II specimens when comparing Tables 4 and 5. In general, shear bond failure was observed for most of the specimens except for the specimens with 900 mm shear span which behaved similar to an under-reinforced concrete beams with flexural failure. The shear bond coefficients and the corresponding regression lines for the G90 and S specimens are shown in Figs. 5 and 6, respectively. The prediction of the shear bond loads, V_s, for the test specimens by the regression equation is shown in Table 5. As can be seen from the table that shear bond loads, V_s, for the test specimens are well within the range of 15%. In addition, the test results of the specimens with 675 mm shear span, which serves as a check on the shear-bond equation, agree very well with the predictions by the shear-bond equation developed from the regression analysis.

DISCUSSION OF TEST RESULTS

Effects of Chevron Shear Key Depth

The average depth of the chevron shear keys for the Phase II specimens was approximately 75% deeper than that of the Phase I specimens. This increase in the shear key depth contributed to an increase in the ultimate load of the specimens as shown in Fig. 7. This figure shows that the

ultimate load of specimen 636-22-900-NE-G90 was increased by more than two times for the same specimens using the steel deck with deeper shear key. Wright et al. (1987) showed that a reduction of approximately 30% in embossment height could result in a drop of load carrying capacity of the specimen by 50%. In addition, the flexural stiffness of the specimen was also increased as shown in the figure. Although the test results of other specimens in Phase II cannot be directly compared with that of Phase I due to the difference in slab thickness, it is believed that the significant increase in ultimate load of the Phase II specimens was mainly due to the increase in the shear key depth.

Effects of Steel Deck Surface Coating

The load deflection curves of specimens 636-22-100-675-NI-S and 636-22-100-675-NI-G90 from Phase I are shown in Fig. 8. These two specimens are identical except the steel deck surface coating and the depth of the indentation (height of embossment). As can be seen in the figure the ultimate load of the S specimen was about 2.5 times that of the G90 specimen Therefore, it is believed that the steel deck surface has a significant effect on the ultimate strength of the specimen. It should be noted that the depth of the indentation of the S specimen was 19% more than that of the G90 specimen, therefore, the significant increase in ultimate strength of the S specimen had to include the effects of both the steel deck surface coating and the measured depth of the indentation. The importance of the surface coating could also be shown by examining the pictures of steel deck surface of the failed specimens as shown in Fig. 9. The top part of the figure shows that significant amount of concrete was still bonded onto the steel deck surface of the failed S specimen. On the other hand, the steel deck surface of the failed G90 specimen showed a smooth and shiny surface as illustrated in the bottom part of the figure. Hence, it is believed that concrete surface developed stronger chemical bond with S coating then with G90 coating.

When examining the test results of Phase II it was observed that the increase in ultimate load due to the effects of surface coating was not as pronounced as that of the test results from Phases I. This is probably due to the significant increase in the mechanical interlocking strength with deeper shear key. It can be seen from the test results of Phase II that this increase in mechanical interlocking strength has a more dominant effect on the ultimate load of the specimens than the increase in chemical bond due to the deck surface coating. Besides, the shear bond strength of the composite slab should not be relied on the chemical bond between the steel deck and the concrete slab.

Effects of Types of Chevron Shear Key

The effects of types of chevron shear key (embossment vs. indentation) are illustrated typically in Fig. 10. This figure shows that indentations increased the shear bond strength and stiffness of the specimens although the depth of the chevron key for the specimens with embossment was 4% to 14% more than that of specimens with indentations. The increase in shear bond strength due to the presence of indentations varies from 7% (14% less in shear key depth) to 15% (4% less in shear key depth). Therefore, it can be seen that if both specimens had the same shear key depth, then, the effects of the types of chevron shear key would be more pronounced. Conversely, however, specimens 636-22-100-675-II-S and 636-22-100-675-IE-S shows that embossment produced higher shear bond strength . This contradiction could be explained by the fact that the shear key depth of specimen 636-22-100-675-IE-S was 24% more than that of specimen 636-22-100-675-II-S. Therefore, it is believed that this significant increase in shear bond strength of the specimen with embossment was caused by the effects of the shear key depth. Further study is necessary to quantify the effects of embossment vs. indentation. Nevertheless, it can be concluded that the indentation shear keys perform similar to the embossment ones.

Effects of Steel Deck Position

The effects of steel deck position (normal vs. inverted) are illustrated in Fig. 11. As can be seen from this figure that the specimen with inverted deck had a lower ultimate load but higher stiffness than that of the specimen with normal deck. Again, this increase in 19% of shear bond strength might be due to the effects of both the position of steel deck and the depth of the chevron shear key. The chevron shear key depth of specimen 636-22-100-675-NI-S was 19% more than that of specimen 636-22-100-675-NI-S , hence, this might have significant effect on the shear bond strength of the specimens. The higher stiffness of the specimen 636-22-100-675-II-S could be explained by the fact that the inverted deck provided more steel area at the bottom of the specimen where tensile reinforcement is more effective. On the whole, the effects of the steel deck position on the shear bond strength of the specimen could not be fully examined by this series of tests. More tests should be performed in order to investigate this factor.

Effects of Shear Span

The effects of shear span on the ultimate strength of the specimens are illustrated typically in Fig. 12. As expected, the stiffness of the specimens increased with decreasing span length. However, the change in ultimate load of the specimens may not be proportional to the change in the span length. Nevertheless, the ultimate strength of the specimens increased with decreasing span length. It should be noted that the S specimens produced more consistent load deflection behavior as illustrated in Fig. 13. The occurrence of this load deflection behavior may be due to the fact that the ultimate strength of the specimens was contributed basically by the chemical bond between the concrete slab and the steel deck. This can be observed from the load end slip curves of these specimens which showed that very negligible end slip of the specimens had occurred before ultimate load was reached.

Failure Mechanism

Based on the general behavior of the test specimens, the following failure mechanism of the composite slab is assumed:

At initial stage (no crack), the steel deck acts compositely with the concrete slab. As load increases, the bending moment is sufficient to induce flexural cracks in the maximum region near the line load. Assuming initial chemical bond is destroyed, the composite action requires both the transfer of horizontal and vertical shearing forces due to the bending moment. At the flexural crack location, there is no shear bond between the steel deck and the concrete slab.

As load increases and at the crack location, the tensile force exists in the steel deck produces relative movement between the steel deck and the concrete slab. The mechanical interlocking strength at this location may be exceeded and the concrete slab may ride slightly up and over the chevron shear key which in turn disengage the shear keys from the concrete slab and the mechanical interlocking strength is reduced. However, frictional force may exist at this location due to the transverse load. As observed from the tests that diagonal crack occurred following the flexural crack. The internal forces at this diagonal crack location are similar to the reinforced concrete member without shear reinforcement. The shear is transferred at the concrete compression zone, the diagonal crack due to aggregate interlocking and the dowel action of the steel deck.

When approaching the ultimate shear bond load of the composite slab, a significant number of shear keys near the original crack location may have been disengaged from the concrete slab such

that the frictional force at this particular location is reduced. The whole process is that at the location (diagonal crack) where both the mechanical and frictional forces are lost, more load is transferred to the nearby shear keys; eventually, the mechanical interlocking strength of those nearby shear keys is reduced and the frictional resistance will be engaged. When this frictional resistance is overcome, the load will be shifted again to the nearby shear keys. This entire process continues until the remaining number of engaged shear keys in the shear span is reduced to a critical level such that the complete concrete slab in the shear span will ride up and over the shear keys and producing large end slips. The final process usually involves diagonal cracks which are extended to the top of the concrete surface. It should also be noted that the as the diagonal crack progressed, a significant part of the shear may be transferred by the dowel action of the steel deck. This dowel force may help to disengage the steel deck from the concrete slab at the final stage.

Based on this assumed failure mechanism, it can be seen that the shear bond strength of the composite slab involves both the transfer of the horizontal shearing force, the vertical force (which affects the frictional force) and the effects of dowel force on the steel deck. However, the moment equilibrium at the cracked section requires that the applied moment due to the transverse load about the length of the shear span has to be balanced by the moment resistance of the composite section as discussed by Schuster and Ling (1980). Hence, the tensile force on the steel deck can be estimated by dividing the moment at ultimate (product of ultimate load and the shear span) by the internal moment arm of the section which is usually defined as (d - a/2) where d is the effective depth of the section and a is the height of the compressive stress block as shown in Fig. 14. If we further assume that the average shear stress distribution at ultimate along the shear span is uniform (Daniels 1988), then the average shear stress τ_{ave} can be calculated by dividing the tensile force by the shear span area. The shear span area is defined as the product of the length of the shear span and the width of the composite slab. The τ_{ave} for the phase II specimens are shown in Table 5. These average shear stress will be compared with the average shear stress evaluated from the pull-out specimens in the following section.

Pull-Out Test Results

The test results for the pull-out specimens are shown in Table 6. It can be seen from the table that for the phase I pull-out specimens with shallow shear keys the pull-out load, P_s, was affected significantly by the pulling direction. The test results show that the pull-out load was increased when the pulling direction was the same as the chevron key direction for the NE type specimens. However, for the NI and II type specimens the pull-out load was increased when the pulling direction was opposite to the chevron key direction. These observations also confirm the recorded failure mode of the slab tests which usually occurred in the weak direction. This behavior can probably be explained by the fact that the sharp edges were produced at the shear keys during the manufacturing process. It was found that for the NE type specimens, sharp edges were located at the inside corner of the chevron key as shown in Fig. 2. Hence, when the pulling direction is such that the concrete slab will bear against the sharp edges the pull-out load of the specimens will be increased. Therefore, it is important to identify the orientation of the shear key if the embossment is not symmetrical. Load vs. end slip curves illustrating the effects of pulling direction is shown in Fig. 15.

The type of shear keys (embossment vs. indentation) did not show significant effects on the pull-out load of the specimens and the load-slip behavior. The surface coating showed appreciable effects on the pull-out load. The load vs. end slip curves for the NE type specimens in the weak direction for both surface coatings are shown in Fig. 16. It can be seen from this figure that the S coating specimen produced higher pull-out load, however, the behavior was relatively brittle.

The pull-out test results for Phase II specimens which have deeper chevron shear key are also shown in Table 6. It can be seen from this table that the pulling direction has no appreciable effects

on the pull-out load of the specimens. In addition, the S coating did not seem to increase the pull-out load. When comparing Phase II pull-out test results to that of Phase I it can be seen that a significant improvement in pull-out load was observed for the Phase II specimens. Hence, it is believed that the increase in mechanical interlocking strength by increasing the depth of the shear key would overcome the effects of other factors such as the surface coating.

As discussed from the above, the average shear stress, τ_{ave}, from the slab test results will be used to compare with that from the pull-out tests. The average shear stress from the Phase II pull-out test τ_{pave} are shown in Table 6 and the τ_{ave} from the Phase II slab tests are shown in Table 5. It can be seen from these tables that the τ_{pave} are in general lower than the corresponding slab test specimens. The slab test results show that τ_{ave} increased with decreasing shear span. Based on these two observations, it is believed that the difference in predictions of the average shear stress from the pull-out tests and the slab tests is mainly due to the effects of the transverse load. When the transverse load is increased the internal friction between the concrete slab and the steel deck is also increased. Hence, the shear bond strength of the composite slab will also be increased. Therefore, it is believed that the predictions of the average shear stress by the pull-out tests can be improved by including the effects of the transverse load.

Conclusions

It can be seen that the shear bond strength of the composite slab specimens increases significantly with increasing depth of the chevron key. The depth of chevron key was also found to be the dominant factor that influenced the behavior of the composite slab specimens. For the particular embossment (chevron shear key) investigated in this study, it was found that the shear bond failure will always initiate in the weak chevron key direction as discussed. The light zinc coating ($75g/m^2$ - S) seems to create a stronger chemical bond with the concrete. However, the shear bond strength of the composite slab should not be relied on the chemical bond.

Lower average shear stress was recorded for the pull-out test specimens when comparing with the slab test results. It is believed the effects of transverse load on the internal friction between the concrete slab and the steel deck, which were not included in the pull-out test setup, contributed to the lower prediction of the average shear stress by the pull-out tests. A better estimate of the pull-out average shear stress for this particular steel deck profile can be obtained if the transverse load effects are incorporated.

Table 1 Average Measured Dimensions of Steel Decks for Phase I

Phase I								
Specimen	b (mm)	B_b (mm)	B_t (mm)	d_d (mm)	t (mm)	C_s (mm)	Flute Angle (θ)	Key Depth (mm)
636-22-100-900-NE-G90	908.0	43.6	84.5	36.9	0.74	153.4	-	1.42
636-22-100-900-NE-G90	910.0	42.5	91.0	37.2	0.78	151.0	70.0	1.34
636-22-100-675-NE-G90	906.0	43.0	90.0	37.7	0.78	152.8	69.0	1.35
636-22-100-450-NE-G90	917.5	41.8	86.7	36.5	0.69	154.0	-	1.14
636-22-100-900-NI-G90	906.0	42.5	90.5	38.6	0.78	151.5	70.0	1.36
636-22-100-675-NI-G90	905.0	43.2	89.5	38.2	0.78	151.2	70.0	1.19
636-22-100-900-II-S	909.0	85.8	44	37.5	0.71	153.0	-	1.38
636-22-100-675-II-S	910.0	42.3	85.3	36.5	0.69	153.8	66.0	1.15
636-22-100-450-II-S	909.0	83.9	43.3	39.2	0.70	153.0	-	1.30
636-22-100-675-NI-S	906.0	42.0	85.3	38.2	0.77	151.8	70.0	1.43
636-22-100-675-IE-S	905.0	41.3	89.3	38.0	0.76	151.8	70.0	1.49

Table 2 Average Measured Dimensions of Steel Decks for Phase II

Specimen	Phase II							
	b (mm)	B_b (mm)	B_t (mm)	d_d (mm)	t (mm)	C_s (mm)	Flute Angle (θ)	Key Depth (mm)
636-22-100-900-NE-G90	897	39.3	88.2	37.5	0.81	152.3	69.2	2.25
636-22-100-900-NE-G90	895	40.0	88.0	37.5	0.80	151.7	68.3	2.28
636-22-125-675-NE-G90	895	39.0	88.5	37.3	0.81	152.7	69.3	2.43
636-22-125-675-NE-G90	895	39.5	88.2	37.2	0.80	152.7	69.2	2.43
636-22-150-450-NE-G90	896	39.0	88.3	37.0	0.82	152.3	69.3	2.34
636-22-150-450-NE-G90	900	39.2	88.5	37.2	0.80	152.3	70.0	2.34
636-22-100-900-NE-S	925	38.5	86.2	36.0	0.75	153.7	68.8	2.21
636-22-100-900-NE-S	925	38.5	85.7	36.5	0.76	153.0	68.8	2.36
636-22-125-675-NE-S	925	38.2	88.7	35.8	0.76	153.0	69.5	2.23
636-22-125-675-NE-S	930	38.5	86.3	36.0	0.75	153.7	68.7	2.46
636-22-150-450-NE-S	930	38.5	88.0	36.2	0.76	153.0	68.8	2.34
636-22-150-450-NE-S	930	38.3	87.5	36.5	0.77	153.0	69.3	2.31

Table 3 Average Measured Dimensions of Steel Decks for Pull-Out Specimens

	Specimens	b (mm)	B_b (mm)	B_t (mm)	d_d (mm)	t (mm)	Cs (mm)	L (mm)	Flute Angle
	1A-NE-G90	440	43	86	36	-	155	912	68°
	1B-NE-G90	441	42	84	37	0.743	154	912	68°
	2A-NE-G90	440	43	83	35	-	156	912	68°
	2B-NE-G90	435	43	85	35	0.770	154	913	70°
	3A-II-G90	442	43	85	36	0.773	154	913	68°
	3B-II-G90	440	42	84	36	0.753	156	914	70°
	4A-II-G90	440	44	85	37	0.767	155	910	70°
Phase	4B-II-G90	440	44	86	37	0.780	154	915	72°
I	5A-NI-G90	442	43	86	37	0.770	150	905	70°
	5B-NI-G90	435	43	87	37	0.790	155	905	72°
	6A-NI-G90	440	41	88	37	0.770	152	907	70°
	6B-NI-G90	435	41	87	37	0.765	152	906	70°
	7A-NE-S	436	42	88	36	0.760	151	910	71°
	7B-NE-S	433	43	86	36	0.751	151	908	72°
	8A-NE-S	440	42	87	37	0.755	153	907	70°
	8B-NE-S	441	41	85	35	0.74	151	908	70°
	9A-NE-G90	441	42	85	36	0.795	155	912	68°
	9B-NE-G90	436	41	85	35	0.801	154	912	68°
Phase	10A-NE-G90	435	43	86	36	0.810	156	912	68°
II	10B-NE-G90	442	42	84	35	0.800	154	913	70°
	11A-NE-S	442	43	86	37	0.765	153	910	70°
	11B-NE-S	441	43	83	37	0.753	154	911	68°
	12A-NE-S	439	41	85	35	0.775	155	913	69°
	12B-NE-S	436	43	85	36	0.770	155	912	69°

Table 4 Test Results for Phase I

Phase I					
Specimen	Fy (MPa)	f'c (MPa)	P_u (kN)	Self-Weight (kN)	V_u (kN/m)
636-22-100-900-NE-G90	277	24.2	13.7	5.93	10.8
636-22-100-900-NE-G90	306	29.2	11.2	6.05	9.50
636-22-100-675-NE-G90	282	31.9	15.3	4.57	11.0
636-22-100-450-NE-G90	279	28.1	33.6	3.24	20.1
636-22-100-900-NI-G90	321	29.7	13.7	6.07	10.9
636-22-100-675-NI-G90	303	29.0	16.7	4.49	11.7
636-22-100-900-II-S	248	23.8	22.6	6.66	16.1
636-22-100-675-II-S	308	31.2	34.5	5.23	21.8
636-22-100-450-II-S	252	25.1	55.6	3.63	32.6
636-22-100-675-NI-S	297	31.2	42.5	4.59	26.0
636-22-100-675-IE-S	287	31.2	53	5.43	32.3

Table 5 Comparison of Test Results to Regression Analysis for Phase II

Phase II								
Specimen	Fy (MPa)	f'c (MPa)	P_u (kN)	Self Weight (kN)	V_u (kN/m)	V_s (kN/m)	$\frac{V_u}{V_s}$	τ_{ave} (MPa)
636-22-100-900-NE-G90	269	33.3	31.9	5.90	21.1	20.9	1.01	0.296
636-22-100-900-NE-G90	290	33.3	31.4	5.88	20.8	21.0	0.99	0.292
636-22-125-675-NE-G90	290	32.1	55.0	5.83	34.0	32.5	1.05	0.353
636-22-125-675-NE-G90	277	32.1	49.2	6.01	30.8	32.5	0.95	0.320
636-22-150-450-NE-G90	285	33.3	89.2	5.10	52.6	52.4	1.00	0.434
636-22-150-450-NE-G90	292	33.3	88.6	5.00	52.0	52.3	0.99	0.429
636-22-100-900-NE-S	269	30.8	34.3	6.07	21.8	22.1	0.99	0.304
636-22-100-900-NE-S	277	30.8	35.3	6.24	22.5	22.2	1.01	0.314
636-22-125-675-NE-S	262	30.8	61.5	6.18	36.6	33.4	1.10	0.378
636-22-125-675-NE-S	262	30.8	57.1	6.18	34.0	33.4	1.02	0.351
636-22-150-450-NE-S	277	30.5	82.2	5.17	47.0	51.4	0.91	0.386
636-22-150-450-NE-S	280	30.5	98.5	5.14	55.7	51.5	1.08	0.457

Table 6 Test Results for Phase I and II Pull-Out Specimens

	Specimen	Pull and Key Direction	Depth of Key (mm)	Number of Keys	Weight of Concrete Slab (kN)	P_s (kN)	τ_{pave} (MPa)
Phase I	1A-NE-G90	◄—►>	1.66	34	0.618	41.3	0.123
	1B-NE-G90	◄—►>	1.65	33.5	0.625	43.3	0.129
	2A-NE-G90	◄—►<	1.38	33.5	0.616	23.9	0.071
	2BNE-G90	◄—►<	1.57	33.5	0.636	23.2	0.070
	3A-II-G90	◄—►>	1.68	34	0.714	20.7	0.061
	3B-II-G90	◄—►>	1.40	34	0.740	24.1	0.072
	4A-II-G90	◄—►<	1.53	33	0.718	59.0	0.176
	4B-II-G90	◄—►<	1.51	33.5	0.718	58.8	0.175
	5A-NI-G90	◄—►<	1.29	33	0.627	49.6	0.149
	5B-NI-G90	◄—►<	1.69	33.5	0.620	46.9	0.143
	6A-NI-G90	◄—►>	1.45	34	0.627	23.0	0.069
	6B-NI-G90	◄—►>	1.33	33.5	0.625	21.2	0.064
	7A-NE-S	◄—►>	1.58	34	0.645	51.6	0.155
	7B-NE-S	◄—►>	1.32	34	0.625	60.1	0.183
	8A-NE-S	◄—►<	1.30	34	0.623	24.6	0.075
	8B-NE-S	◄—►<	1.46	34	0.616	33.5	0.101
Phase II	9A-NE-G90	◄—►>	2.27	33	0.618	72.4	0.220
	9B-NE-G90	◄—►>	2.52	33	0.625	74.6	0.228
	10A-NE-G90	◄—►<	2.32	33	0.616	73.5	0.223
	10B-NE-G90	◄—►<	2.43	33	0.605	69.2	0.210
	11A-NE-S	◄—►>	2.13	33	0.592	-	-
	11B-NE-S	◄—►>	2.00	33	0.609	58.2	0.176
	12A-NE-S	◄—►<	2.32	32	0.623	59.9	0.180
	12B-NE-S	◄—►<	2.23	32	0.623	60.4	0.183

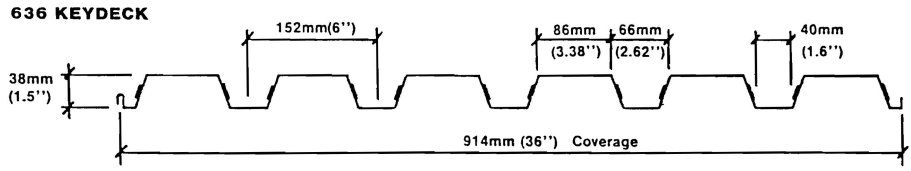

Figure 1 Schematic of 636 Steel Deck

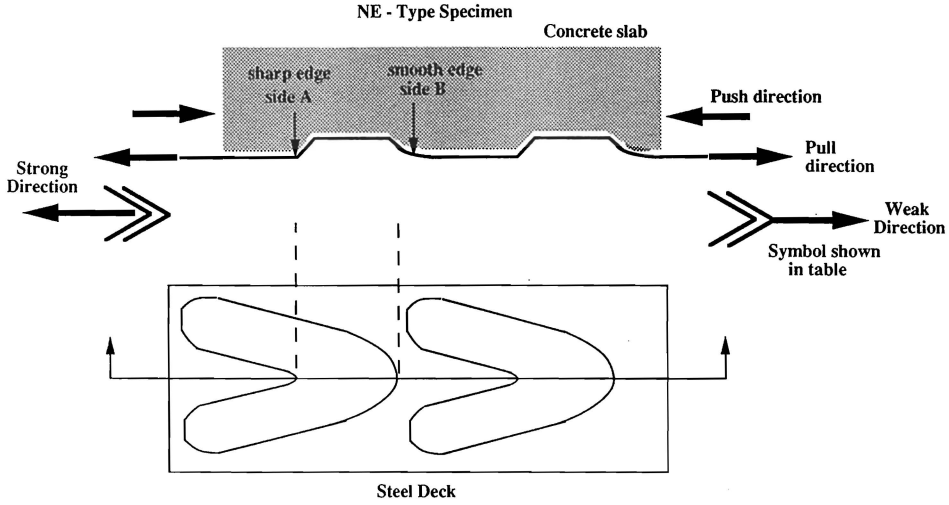

Figure 2 Schematic of Pull Direction for Pull-Out Specimens

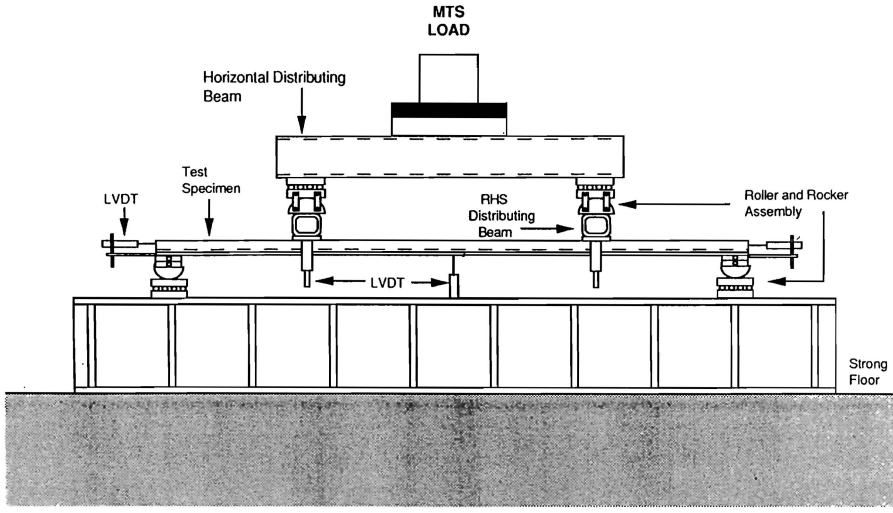

Figure 3 Schematic of One-Way Slab Test Setup

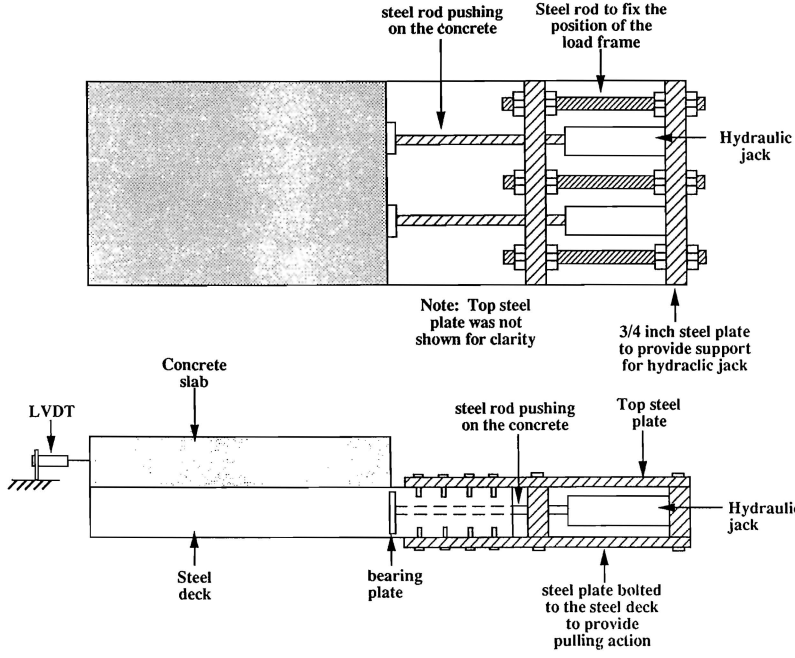

Figure 4 Schematic of Pull-Out Test Setup

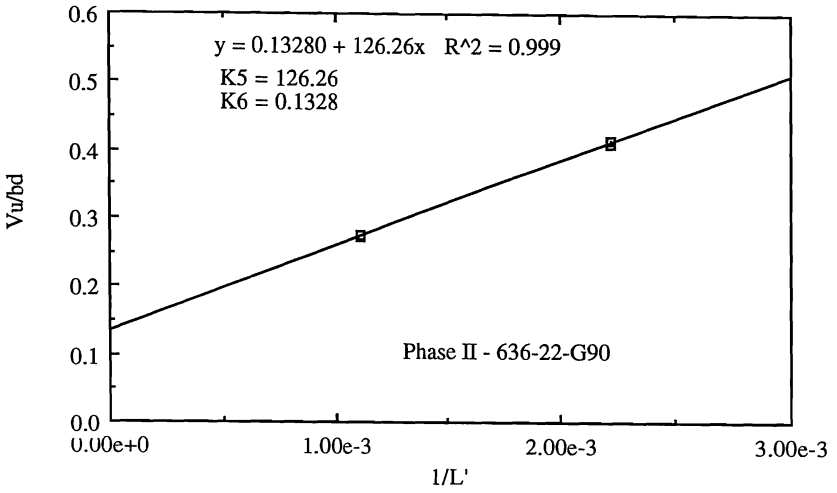

Figure 5 Regression Line for 636-22-G90 Steel Deck

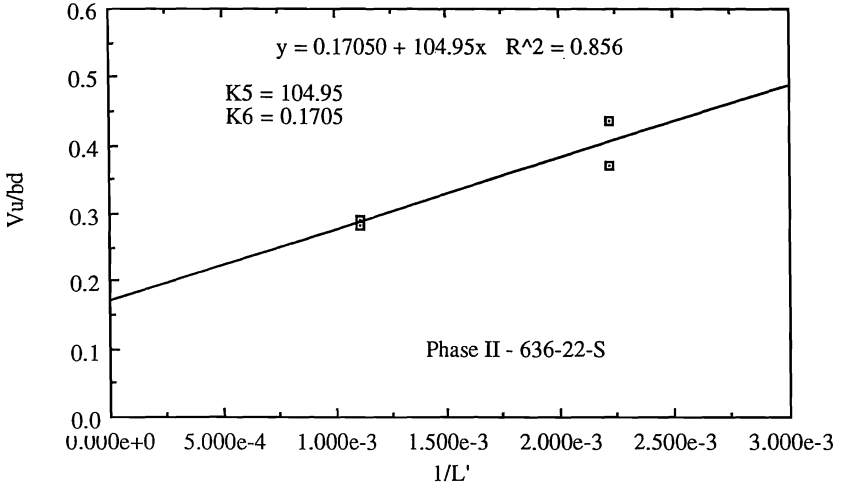

Figure 6 Regression Line for 636-22-S Steel Deck

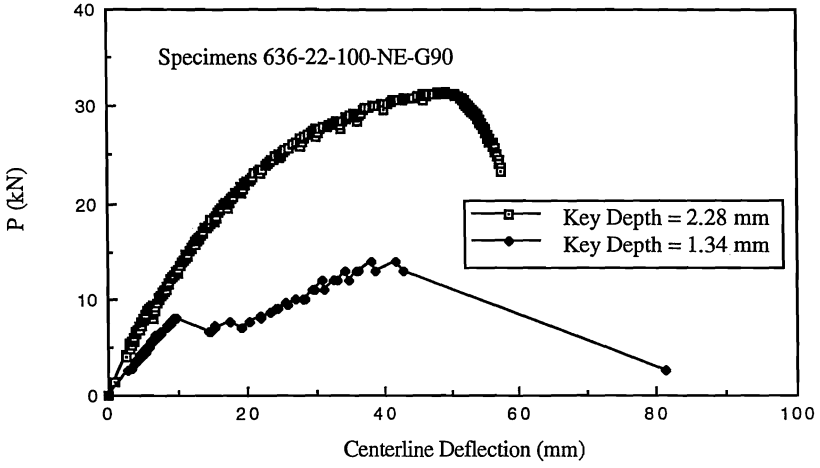

Figure 7 Effects of Chevron Key Depth on Load Deflection Behavior of Composite Slab

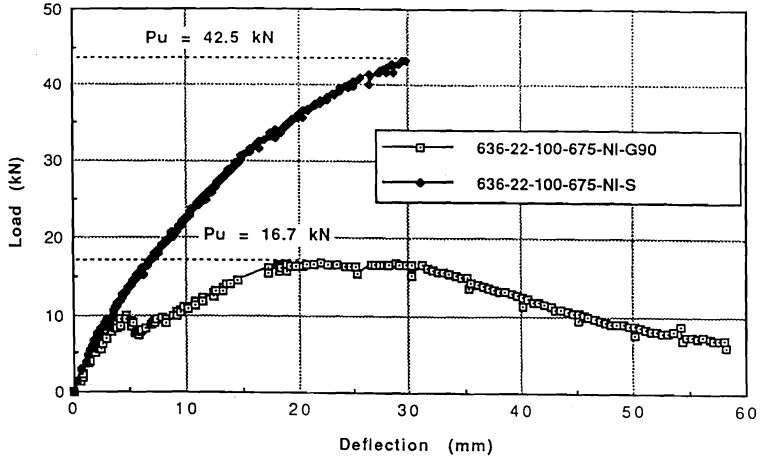

Figure 8 Effects of Deck Surface Coating on Load Deflection Behavior of Composite Slab

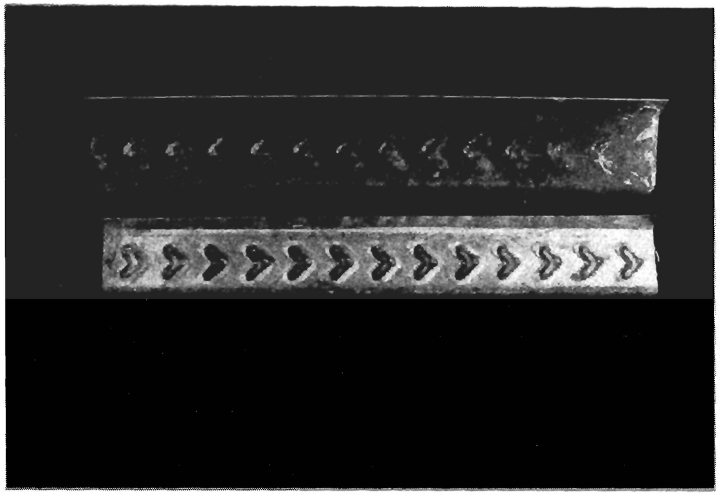

Figure 9 Typical Steel Deck Surface of Failed Specimens

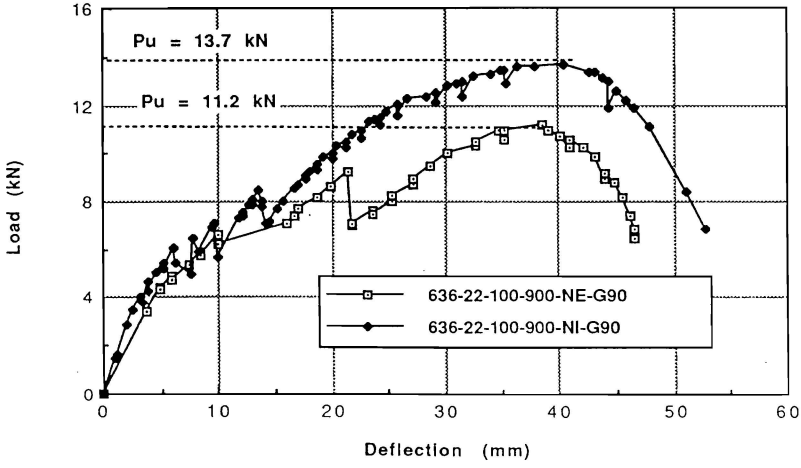

Figure 10 Effects of Types of Chevron Shear Key on Load Deflection Behavior of Composite Slab

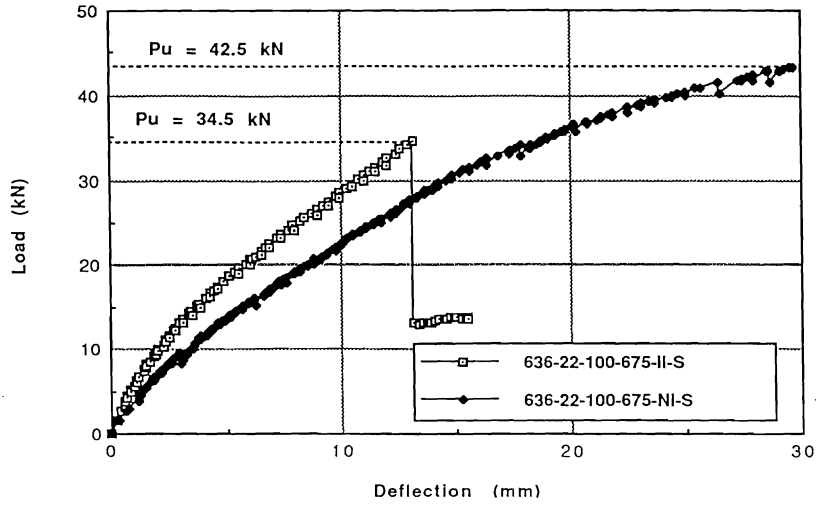

Figure 11 Effects of Steel Deck Poistion on Load Deflection Behavior of Composite Slab

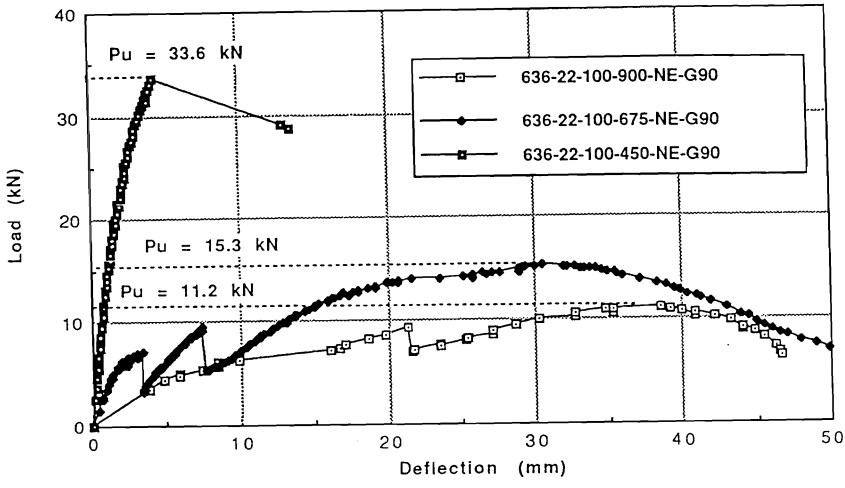

Figure 12 Effects of Shear Span Length on Load Deflection Behavior of Composite Slab for G90 Coating Specimens

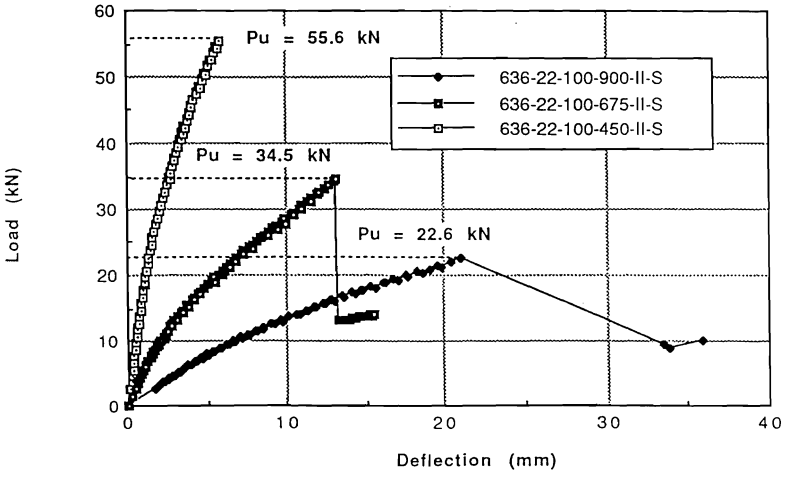

Figure 13 Effects of Shear Span Length on Load Deflection Behavior of Composite Slab for S Coating Specimens

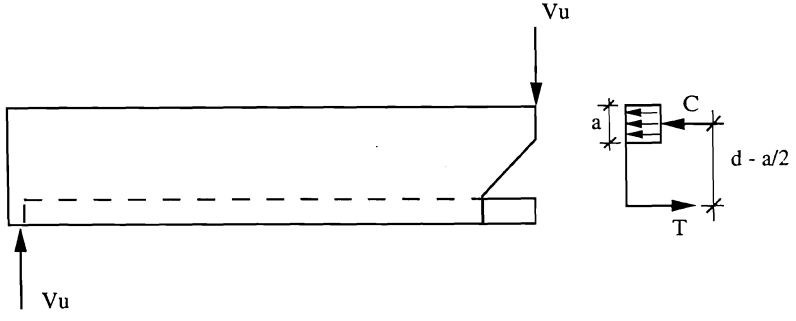

Figure 14 Internal Forces at Cracked Section for Moment Equilibrium

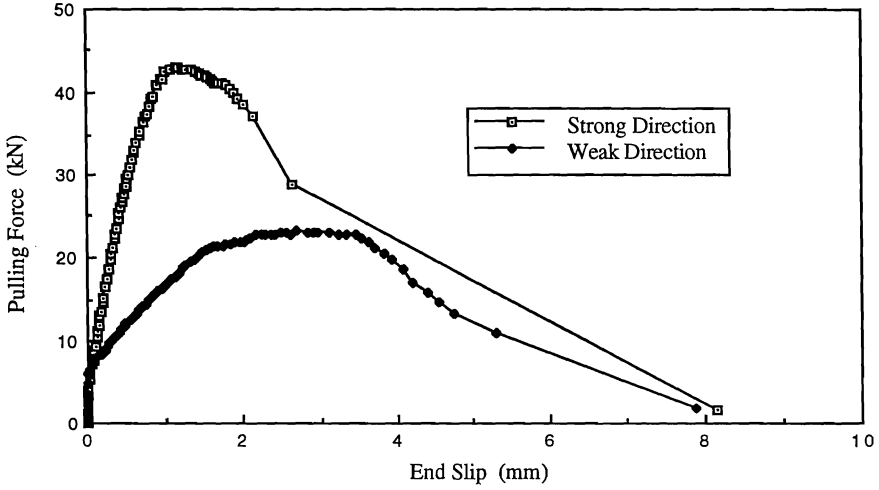

Figure 15 Effects of Pulling Direction on the Curves of Pulling Forces vs. End Slip

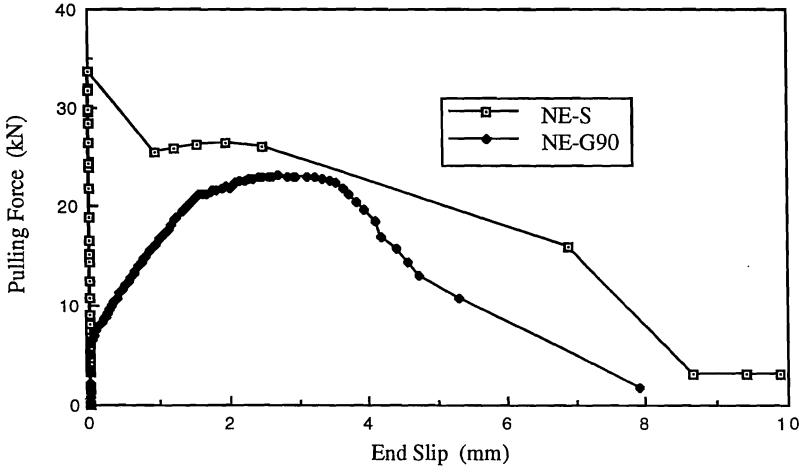

Figure 16 Effects of Deck Surface Coating on Pulling Force vs. End Slip Curves

APPENDIX -- REFERENCES

CAN3-A23.3-M84, 1984. Design of Concrete Structures for Buildings, Canadian Standards Association, Rexdale, Ontario, Canada.

CSSBI S3-88, 1988. Criteria for the Testing of Composite Slabs, Canadian Sheet Steel Building Institute, Willowdale, Ontario, Canada.

CSSBI S2-85, 1985 (Revised 1988). Criteria for the Testing of Composite Slabs, Canadian Sheet Steel Building Institute, Willowdale, Ontario, Canada.

Daniels, B.J. 1988. "Shear Bond Pull-Out Test fro Cold-Formed-Steel Composite Slabs." Ecole Polytechnique Federale De Lausanne. (Publication ICOM 194).

Daniels, B.J. and Crisinel M. 1992. "Composite Slab Behavior and Strength Analysis. Part I: Calculation Procedure." Journal of Structural Engineering, ASCE, Vol. 119, No.1, pp. 16-35.

Daniels, B.J. and Crisinel M. 1992. "Composite Slab Behavior and Strength Analysis. Part II: Comparisons with Test Results and Parametric Analysis." Journal of Structural Engineering, ASCE, Vol. 119, No.1, pp. 36-49.

Jolly, C.K. and Zubair, A.K.M. 1987. "The Efficiency of Interlocking Between Profiled Steel Sheeting and Concrete." In: Concrete Steel Structures Advances, Design and Construction. Elsevier Applied Science, London, pp. 127-136.

Porter, M.L., Ekberg, C.E., Greimann, L.F., and Elleby, H.A. 1976. "Shear Bond Analysis of Steel-Deck Reinforced Slabs." Journal of the Structural Division, ASCE, Vol. 102, ST5, pp. 899-917.

Schuster, R.M. 1990. "636 Keydeck Composite Slab System." University of Waterloo Research Institute. Report No. WRI 636-90.

Schuster, R.M. and Ling, W.C. 1980. "Mechanical Interlocking Capacity of Composite Slabs." Proceedings of the Fifth International Specialty Conference on Cold-Formed Steel Structures, University of Missouri-Rolla, pp. 387-403.

Seleim, S.S. and Schuster, R.M. 1982. "Shear-Bond Capacity of Composite Slabs." Proceedings of the Sixth International Specialty Conference on Cold-Formed Steel Structures, University of Missouri-Rolla, pp. 511-531.

Specification for the Design and Construction of Composite Slabs. 1984. ASCE Standard, ASCE, New York, N.Y.

Wright, H.D., Evans, H.R. and Harding, P.W. 1987. "The Use of Profiled Steel Sheeting in Floor Construction." Journal of the Construction Steel Research. Vol. 7, pp. 279-295.

APPENDIX -- NOTATION

a	Depth of concrete compression stress block
b	Width of composite slab
B_b	Width of bottom flange of steel deck
Bt	Width of top flange of steel deck
Cs	Cell spacing of steel deck
d	Effective slab depth - distance from the top of the concrete slab to the centroid of the steel deck
dd	Depth of steel deck
L	Length of pull-out test specimens
L'	Shear span length of one-way slab test specimen
t	Steel deck thickness
f'c	Compressive concrete cylinder strength
Fy	Static yield strength of the steel deck material
Ps	Ultimate applied load of pull-out test specimen
Pu	Ultimate applied load of one-way slab test specimen
Vs	Shear-bond load predicted by regression analysis per unit width of slab
V_u	Experimental shear bond load per unit width of slab
θ	Flute angle of steel deck
τ_{ave}	Average shear stress in the shear span for the one-way slab test specimen
τp_{ave}	Average shear stress in pull-out test specimen